A Small-Satellite Demonstrator for Generating Artificial Gravity in Space via a Tethered System

Andre P. Mazzoleni*and John H. Hoffman†

Abstract

It is well-known that prolonged exposure in humans to a microgravity environment leads to significant loss of bone and muscle mass; this presents a formidable obstacle to human exploration of space, particularly for missions requiring travel times of several months or more, such as a 6 to 9 month trip to Mars. Artificial gravity may be produced by spinning a spacecraft about its center of mass, but since the g–force generated by rotation is equal to "omega-squared times r" (where omega is its angular velocity and r is the distance from the center of rotation), we have that unless the distance from the center of rotation is several kilometers, the rotation rate required to generate "$1-g$" would induce vertigo in the astronauts as they moved about the capsule (e.g. if the distance from the center of rotation is 10 meters, the required rotation rate for $1-g$ would be 9.5 rpm). By tethering the crew capsule to an object of nearly equal mass (such as the spent final rocket stage) at a distance of 1 to 2 kilometers, the necessary rotation rate would be sufficiently small as to not cause discomfort for the astronauts. For example, if the distance from the center of rotation is 2 kilometers, the required rotation rate for $1-g$ would be 0.67 rpm; at 1 kilometer the rate is still only 0.95 rpm. 1 rpm is considered an acceptable spin rate for the human body to withstand for extended periods of time. This paper gives an overview of the Tethered Artificial Gravity (TAG) satellite program, a 2-part program to study the operation and dynamics of an artificial-gravity-generating tethered satellite system. Phase I of the program will culminate in a flight of a model spacecraft in a non-ejected Get-Away-Special (GAS) Canister on the Space Shuttle. It is to be operated under the aegis of the Texas Space Grant Consortium. The purpose of the Phase I flight is to test key components of the system to be flown in Phase II of the program. Phase I will also involve detailed modeling and analysis of the dynamics of the spacecraft to be flown in Phase II of the program; the Phase II spacecraft will be a small, 65 kg, tethered satellite system which will be boosted into low-earth orbit, deployed and then spun-up to produce artificial gravity. In addition to a description of the TAG program, results of parametric studies related to TAG will be presented in this paper.

Introduction

A manned mission to mars presents numerous challenges, such as: developing a propulsion system capable of sending the crewed vehicle and its supplies to Mars; providing a system architecture capable of returning the crew safely to Earth at the conclusion of the mission; providing habitation and life support systems for the crew while on Mars; and protecting the crew from the harsh radiation environment of space while in transit to Mars.

While the challenges outlined above are significant, various efforts are underway to meet these challenges, or to lay the groundwork for meeting these challenges. Research into a variety of advanced propulsion systems is currently being undertaken by NASA, private industry and other government space agencies, and while progress has been slow, it is nonetheless an active area of research. NASA is also continuing to work on its Mars mission architecture, concentrating on a "Mars-direct" approach which involves manufacturing

*Associate Professor, Department of Engineering, Texas Christian University, Box 298640, Fort Worth, TX 76129; 817/257/6317; a.mazzoleni@tcu.edu

†Professor and Head, Physics Programs, University of Texas at Dallas, P. O. Box 830688, Richardson, TX 75083-0688; 972/883/2846; jhoffman@utdallas.edu

the propellant necessary for the return trip to Earth from resources found on Mars (i.e. in-situ propellant production). In fact, experiments have already been done which demonstrate that in-situ propellant production is feasible. Experiments involving development of closed-system life support systems are underway at Johnson Space Center (JSC) and other locations; JSC has placed crews for extended periods of time inside a closed system, and similar experiments are being conducted at the Biosphere II facility in Arizona. Protection from radiation is a thornier issue, as radiation exposure in space presents a major health hazard; for example, if left unshielded, a crew could easily be killed by the radiation emitted by major solar flares. This problem is being addressed, however, on many fronts. Much work has been done over the past few decades on quantifying the levels of radiation exposure that humans can tolerate and experiments with various methods of shielding have been conducted on the ground and in space, with one of the more promising ideas being to use the crew's water supply as a shield. Shielding continues to be an active area of research.

The purpose of outlining the various challenges discussed above and how they are being addressed is to highlight how much work needs to be done regarding another key challenge of a Manned Mars mission, namely the effect of microgravity on human physiology.

It is well-known that prolonged exposure in humans to a microgravity environment leads to significant loss of bone and muscle mass; this presents a formidable obstacle to human exploration of space, particularly for missions requiring travel times of several months or more, such as a 6 to 9 month trip to Mars[8]. Various remedies involving exercise and diet have been tried during long duration space missions around the Earth (i.e. aboard Skylab, Mir and the International Space Station), but nothing has been able to prevent the loss of bone and muscle mass during lengthy stays in space (although exercise does seem to slow down the rate of loss of muscle mass). The seriousness of this problem is quite apparent when one considers what the crew will be required to do upon arrival at Mars in terms of setting up living quarters, managing life support systems, and embarking on surface exploration missions. If the crew is weak and their bones are brittle due to the effects of microgravity, the chance of having a successful mission would be minimal at best. Thus, the solution of this problem is definitely as critical as any of the other key mission elements, such as propulsion, radiation shielding, etc.

Barring the development of a "miracle-drug" which halts bone and muscle mass losses during exposure to microgravity, the only possible solution is to generate artificial gravity for the crew while in transit to Mars. Artificial gravity may be produced by spinning a spacecraft about its center of mass (CM), but since the g–force generated by rotation is equal to $\omega^2 r$, where ω^2 is its angular velocity and r the distance from the center of rotation, unless the distance from the center of rotation is several kilometers, the rotation rate required to generate one g would induce vertigo in the astronauts as they moved about the capsule (e.g. if the distance from the center of rotation is 10 meters, the required rotation rate for one g would be 9.5 rpm). By tethering the crew capsule to an object of nearly equal mass (such as the spent final rocket stage) at a distance of 1 to 2 km, the necessary rotation rate would be sufficiently small as to not cause discomfort for the astronauts (c.f.[34, 39, 41]). For example, if the distance from the center of rotation is 2 kilometers, the required rotation rate for one g would be 0.67 rpm; at 1 km the rate is still only 0.95 rpm. 1 rpm is considered an acceptable spin rate for the human body to withstand for extended periods of time[8].

To develop this concept, the stability and spin-up dynamics of tethered systems with similar-sized end-masses must be modeled and then tested in space. NASA's TSS and SEDS missions investigated tether dynamics, but for both of these systems there were several orders of magnitude mass difference between the two end-masses. There has been very little work done on systems with nearly equal end-masses. Also, none of these missions involved a "spin-up" of the system, where the tethered end-body was partially reeled-in in order to spin-up the system and create artificial gravity. The authors of this paper have been working on the design of an experimental satellite to test out the concept of using a tethered system to generate artificial gravity. We have spent considerable time generating simulations of such as system and have learned a great deal in the process, but flight experiments are necessary in order to validate the models and to discover unexpected phenomena which may not show up in our simulations; this is, of course, true for any experimental flight system, but is of particular concern in this case because of the highly nonlinear behavior of tethered systems.

The mission proposed by the authors to investigate the use of tethered systems to generate artificial

gravity is the Tethered Artificial Gravity (TAG) satellite program. TAG is a 2-part program toward the development of such a system: Phase I will culminate in a test flight of a tether-deployer and various subsystems in a non-ejected GAS-Canister on the Space Shuttle; Phase II will involve the flight of a small (65 kg) tethered satellite system which will be boosted into LEO, deployed and then spun-up to produce artificial gravity. The remainder of this paper will give an overview of the TAG program along with some of the results of our simulations.

Earlier work on this project produced elementary models and simulations of the separation and spin-up dynamics of the TAG satellite[17, 18, 19, 20, 21, 22]. These deal with the dynamics and motions of the two end-masses after they are separated from each other and the tether is deployed from the tether deployer. In the study of the dynamic motion of the TAG satellite, equations of motion for the system have been generated via standard Lagrangian methods and integrated numerically. The analysis was initially performed by treating the two sections of the satellite as point masses which were connected by a massless tether which was assumed to be inextensible and to remain straight throughout the deployment and retrieval process; the analyses currently underway account for the mass and flexibility of the tether and treat the end-bodies as three dimensional objects (not just as point-masses). The field of tethers in space has been studied extensively over the past 40 years; in the bibliography we present a sampling of the work that has been done in this area in recent decades.

Phase I

The Phase I spacecraft, consists of a hexagonal cylinder (18 in. across and 25 in. long) mounted in the GAS-CAN (a standard model having a sealed cover and no ejection mechanism). TSGC has a GAS-CAN that it has made available to the TAG program. It was purchased and donated to TSGC long ago and has a high priority for flight. The TAG spacecraft structure has been designed using extruded aluminum bars as strength members screwed together at the corners with specially designed three way brackets. Since it has not been flown, it will be outfitted with accelerometers and thermistors to monitor its survival during the powered flight and other maneuvers of the mission. It will contain several video cameras to qualify them for space flight since one will be needed for Phase II when the spacecraft is ejected from the carrier vehicle. The video cameras will monitor student experiments in the spacecraft as needed. Necessary lighting will be provided.

The student experiments are an integral part of the flight since they will represent a significant outreach into the community to instill excitement in younger students for science and space exploration. Student groups will be selected from UTD, TCU in Fort Worth and Lamar University in Beaumont, TX, and secondary schools in Beaumont and the Dallas-Ft. Worth area. A certain volume, weight and power will be allocated to these instruments. Modular box-type sections that fit into the hexagonal sections of the spacecraft body will be made available to the student groups. There will be optional windows in the boxes for video camera monitoring. Data will be stored on-board for retrieval after the flight. Items designed by middle school students will be flown to the extent allowed by the available space.

Phase II

The spin-up maneuver to be demonstrated on orbit in Phase II is designed to show the feasibility of spinning-up a tethered system about its center-of-mass. This is accomplished by reeling onto the deployer reel a portion (up to three quarters) of the tether. The reel will be driven by a motor that is controlled by the on-board computer. As the tether is reeled back in, libration of the system will increase. Coriolis forces acting on the end-masses will produce a rapid increase in the rotational motion of the system causing it to spin end over end about its center-of-mass in a dumbbell fashion. The rotational motion will produce a centripetal acceleration in each end-mass and hence a g–force on the end-masses Modeling of this spin-up process (a Phase I task) is critical to the success of Phase II of the mission because the model will provide a guide for

the amount of tether to be reeled in, the optimum reel-in rate and the optimum way to orient the attitude of the system prior to spin-up in order to develop a 1–g environment.

In order to accomplish the spin-up maneuver of the tethered end-masses that will be demonstrated in Phase II of the program (when the spacecraft is ejected from the GAS-CAN), a test of the spin-up deployer/reel will be conducted in Phase I. A reel-type deployer and a similar unit to take-up the deployed tether will be mounted in the spacecraft. During flight, the tether will be fed from one reel to the other to study the operation of these reels in "$0-g$" (and after they have been exposed to flight accelerations and temperatures). The system will be instrumented with tensiometers and rotation counters. Video recordings will be made of its operation. These reels and motors will be prime candidates for the Phase II spacecraft.

The initial design of the Phase II spacecraft included a large spring that pushed the two end-masses apart with a 5 km/sec separation velocity, but the dynamic analysis showed that under some conditions of attitude the tether would not fully deploy[18]. The design was then changed to substitute a cold-gas thruster system for the spring. Cold-gas thrusters will provide a continuous thrust to separate the end-masses, until they are sufficiently far apart for the gravity gradient force to take over, and will give a gentle controlled separation rather than the sudden impulse a large spring would produce. Up to two km of tether will be deployed from the deployer reel located in one of the end-masses.

Modeling

Due to the complexity of tethered satellite systems, it is often useful to start with simple models to gain physical insight into the problem before progressing to more detailed models. The simplest model assumes that the motion of the system is constrained to the orbital plane, that the center of mass of the system moves in a circular orbit and that the two end-bodies of the system are point masses which are connected by a massless tether which is assumed to be inextensible and to remain straight throughout the deployment and retrieval processes. It should be noted here that even with these simplifying assumptions the system exhibits a very rich range of behaviors. Greater degrees of complexity can be added to this simple model (often called the dumbbell model) by including the effects of tether elasticity, tether mass and by modeling the end-bodies as three dimensional objects instead of as point masses. In addition, the system becomes more complicated if nonplanar motion is considered, i.e. if the system not constrained to librate in the orbital plane. Our approach has been to use standard Lagrangian analysis to derive equations of motion, and then to integrate these equations numerically. We present here the equations of motion for some of the models we have investigated.

Planar Dumbbell Model

If we assume that the motion of the system is constrained to the orbital plane, that the center of mass of the system moves in a circular orbit, and that the tether is massless and inextensible, we have that the equations of motion are given by (c.f. [19]):

$$\ddot{L} - L\left(\dot{\theta}^2 + 2\Omega\dot{\theta} + 3\Omega^2\cos^2\theta\right) = -T_0/\bar{m} \tag{1}$$

$$\ddot{\theta} + 2\frac{\dot{L}}{L}\left(\Omega + \dot{\theta}\right) + \frac{3}{2}\Omega^2\sin 2\theta = 0 \tag{2}$$

where

$\bar{m} = \frac{m_A m_B}{m_A + m_B}$

m_A, m_B = the masses of the two halves of the TAG satellite

L = the distance between m_A and m_B (the length of the tether)

θ = the angle between the tether and the local vertical (i.e. the in-plane libration angle)

$\Omega = \frac{GM_e}{R_0^3}$ = the orbital angular velocity

G = the gravitational constant

M_e = the mass of the Earth

R_0 = the orbital radius of the center of mass of the system

T_0 = tether tension

Nonplanar Dumbbell Model

If we assume that the center of mass of the system moves in a circular orbit, that the tether is massless and inextensible, but do not assume that the motion is constrained to the orbital plane, we have that the equations of motion of the system are given by (c.f. [18, 20]):

$$\ddot{L} - L\left[\left(\dot{\theta}+\Omega\right)^2\cos^2\phi + \dot{\phi}^2 + 3\Omega^2\cos^2\theta\cos^2\phi - \Omega^2\right] = -\frac{T_0}{\bar{m}} \tag{3}$$

$$\ddot{\theta} - 2\left(\dot{\theta}+\Omega\right)\dot{\phi}\tan\phi + 2\frac{\dot{L}}{L}\left(\dot{\theta}+\Omega\right) + 3\Omega^2\cos\theta\sin\theta = 0 \tag{4}$$

$$\ddot{\phi} + 2\frac{\dot{L}}{L}\dot{\phi} + \left[\left(\dot{\theta}+\Omega\right)^2 + 3\Omega^2\cos^2\theta\right]\cos\phi\sin\phi = 0 \tag{5}$$

where

L = the distance between m_A and m_B (the length of the tether)

θ = the "pitch" angle of the tether axis, i.e. the in-plane angle between the tether axis and the local vertical

ϕ = the "roll" angle of the tether axis, i.e. the out-of-plane angle between the tether axis and the local vertical

Planar Dumbbell Model with Elasticity Effects Included

If we return now to the planar dumbbell but include elasticity effects of the tether (we assume here that the tether elasticity is linear), we obtain the following equations of motion (c.f. [22]):

$$\ddot{L} - L\left(\dot{\theta}^2 + 2\Omega\dot{\theta} + 3\Omega^2\cos^2\theta\right) + \frac{EA}{\bar{m}}\epsilon U(\epsilon) = 0 \tag{6}$$

$$\ddot{\theta} + 2\frac{\dot{L}}{L}\left(\Omega+\dot{\theta}\right) + \frac{3}{2}\Omega^2\sin 2\theta = 0 \tag{7}$$

where

L_0 = the unstretched length of the tether

L = the distance between m_A and m_B, i.e. the actual (stretched) length of the tether

E = the modulus of elasticity of the tether

A = the cross sectional area of the tether

$\epsilon = \frac{L-L_0}{L_0}$

$U(\cdot)$ is the Unit Step function (i.e. $U(\epsilon) = 1$ if $\epsilon \geq 0$ and $U(\epsilon) = 0$ for $\epsilon < 0$)

θ = the angle between the tether and the local vertical (i.e. the in-plane libration angle)

Note here that additional complexity could be introduced if nonlinear elastic effects were included.

Planar Inelastic Model with End-Bodies Treated as Three dimensional Objects

To study the dynamics of the end-masses when they are treated as three dimensional objects (i.e. instead of as point masses), we initially assume that the attitude motions of the end-bodies do not affect the deployment and retrieval processes (i.e. we assume that the tether axis moves as if the end-bodies were point masses); this assumption, of course, may not be valid if the attitude motion is severe enough to interfere with the reel-in mechanism. With the aforementioned assumption, we have that the motion of each end-body is the result of the gravity-gradient torque acting on the body and the torque applied by the tether at its point of attachment to the body. We consider here all motion to take place in the orbital plane, and define axes $\vec{e}_1, \vec{e}_2, \vec{e}_3$ to be the principal body axes of the body (with corresponding principal moments of inertia J_1, J_2, J_3) where axis $\vec{e}_2$ is normal to the orbital plane, $\vec{e}_3$ is aligned with the tether when the body is at equilibrium and $\vec{e}_1$ completes the triad. With these axes, we define ℓ_1 and ℓ_3 to be the distance from the center of mass of the body to the tether attachment point along the $\vec{e}_1$ and $\vec{e}_3$ axes, respectively. If we then define β to be the angle that $\vec{e}_3$ makes with the local vertical, then the equation of motion describing the attitude motion of the end-body is given by ([21]):

$$J_2\ddot{\beta} = -1.5\Omega^2 \left(J_3 - J_1\right) \sin 2\beta - \left(\ell_1 \cos\beta + \ell_3 \sin\beta\right) T_0 \cos\theta + \left(-\ell_1 \sin\beta + \ell_3 \cos\beta\right) T_0 \sin\theta \tag{8}$$

where for the deployment case T_0 is a function of the friction in the deployment mechanism and θ and L are found by integrating Eqs.6 and 7, and for the deployment case L is determined by the specified speed of the retrieval reel and θ and T_0 are found by again integrating Eqs.6 and 7.

Simulation Results

In this section we present some of the results of our simulation studies.

Deployment

The deployment analyses presented here were originally presented in Ref.[18] and were performed by using the "Nonplanar Dumbbell Model" equations discussed earlier. (For early work related to this problem, see Refs.[9, 29, 35, 38]).

For the simulations shown below we assume the following values for the orbital parameters, satellite masses and initial separation distance of the mass centers of the two halves of the satellite.

$m_A + m_B = 65$ kg

$R_0 = 6678$ kilometers (300 km above the surface of the Earth) $\Rightarrow \Omega = 0.0011595$ rad/sec

$L\left(0\right) = 0.1$ meters

What we are most interested in is an investigation of how the final deployment length of the system depends on the initial conditions (initial separation velocity, spatial orientation and angular velocities), and the system parameters (the tension, T_0, of the tether and the distribution of masses m_A and m_B). Therefore, we have run multiple simulations of the system, varying the collection of variables of interest (parameters and initial conditions) and plotted the maximum deployment achieved in each case. We are most interested in plotting deployment achieved vs. orientation of the tether axis at the time of separation, so our three-dimensional plots consist of independent variables θ and ϕ on the "x" and "y" axes and deployment achieved as the dependent variable which is plotted along the "z" axis. In creating the plots we set the initial angular velocities $\dot{\theta}\left(0\right)$ and $\dot{\phi}\left(0\right)$ to zero because an earlier study (Ref.[17]) showed that initial angular velocity has little effect on the final deployment length; this is due to the fact that conservation of angular momentum drives the angular velocities to zero shortly after separation occurs (i.e. the rise in system moment of inertia due to the rapid increase in L quickly drives the angular velocities to zero).

Many plots were constructed as part of this study (see Ref.[18]), but space limitations require that we present here only some of the more interesting cases. In Figs. 1–6 we show final deployed length achieved as a function of alignment with the local vertical prior to deployment for the following values of T_0, m_A and $\dot{L}(0)$:

Fig.1: $T_0 = 50$ mN, $m_A = 25$ kg and $\dot{L}(0) = 5.0$ m/sec

Fig.2: $T_0 = 100$ mN, $m_A = 25$ kg and $\dot{L}(0) = 5.0$ m/sec

Fig.3: $T_0 = 100$ mN, $m_A = 25$ kg and $\dot{L}(0) = 4.0$ m/sec

Fig.4: $T_0 = 100$ mN, $m_A = 25$ kg and $\dot{L}(0) = 4.5$ m/sec

Fig.5: $T_0 = 100$ mN, $m_A = 20$ kg and $\dot{L}(0) = 4.5$ m/sec

Fig.6: $T_0 = 100$ mN, $m_A = 30$ kg and $\dot{L}(0) = 4.5$ m/sec

The preliminary design for TAG calls for values of $m_A = 25$ kg and $\dot{L}(0) = 5.0$ m/sec. With these values, Fig. 1 shows that for $T_0 = 50$ mN, we achieve full deployment (2000 meters) for all possible initial alignments of the tether axis. But Fig.2 that for $T_0 = 100$ mN, we do not achieve full deployment unless the tether axis is aligned fairly closely with the local vertical prior to deployment. Tests of the tether deployer in air at room temperature show deployer friction to be $T_0 = 50$ mN, but it is not known what T_0 will be when the tether is exposed to the vacuum and temperature extremes found in orbit. If T_0 turns out to be 100 mN instead of 50 mN, we can see from Fig. 2 that we must deploy with the tether axis aligned fairly closely with the local vertical in order to achieve full deployment.

Using the nominal value $m_A = 25$ kg and assuming that T_0 is off by a factor of 2 ($T_0 = 100$ mN), Figs. 2–4 show the effect of different values of $\dot{L}(0)$ on deployment. The separation spring is designed to provide a separation velocity of 5.0 m/sec, but the spring may behave differently than designed when exposed to the space environment; from Fig. 3 we see that if $\dot{L}(0) = 4.0$ m/sec, full deployment is not achieved even if the tether axis is perfectly aligned with the local vertical. For $\dot{L}(0) = 4.5$ m/sec, we see from Fig.4 that full deployment can be achieved provided the tether axis is aligned fairly closely with the local vertical prior to deployment. (Note that space constraints on-board the satellite limit the size spring which can be used to separate the two halves of the satellite.)

Finally, we examine the effect of mass distribution on deployment. Figs. 4–6 show that the degree of alignment required of the tether axis with the local vertical becomes less critical as we distribute the mass more evenly between the two halves of the satellite (recall that the total mass of the satellite is 65 kg). Of course the degree to which this can be done is limited by other constraints, such as the fact that Shuttle integration requirements specify that the composite center of mass must be within 10 cm of the lower end of the satellite.

We have developed a method for studying the effect of various system parameters and initial conditions on the ability of the TAG tethered satellite system to achieve full deployment of its tether. The analysis shows that achievement of full deployment depends critically on such factors as mass distribution, initial separation velocity, tether tension and alignment of the tether axis with the local vertical prior to deployment.

The fact that for many parameter values under consideration for the mission the tether axis must be closely aligned with the local vertical prior to deployment in order for full deployment to occur led us to conclude that an alternate approach for separation is needed, i.e. that we need to use a cold-gas thruster system instead of a spring to separate the two halves of the satellite.

Retrieval

The retrieval analysis presented here again uses the "Nonplanar Dumbbell Model" equations discussed earlier. For the simulations presented here we assume the following values for the orbital parameters, satellite masses and the length of the tether connecting the two halves of the satellite prior to initiation of the retrieval process.

$m_A = 25$ kg

$m_B = 40$ kg

$\Omega = 0.0011636$ rad/sec (90 minute orbital period)

$L_i = L(0) = 2000$ meters

What we are investigating here is how such factors as the rate of retrieval, final retrieval length, the initial angular velocity and the initial angular position of the system (relative to the local vertical prior to retrieval) will affect the tension induced at the end of the retrieval process.

For the purpose of this study, we have chosen to use a simple exponential control law for the length L of the tether (e.g. as discussed in [23] and [24]), i.e. we specify

$$L(t) = L_i e^{-ct} \tag{9}$$

where

$$c = \frac{\ln(L_i/L_f)}{t_R}$$

and L_i is the length of the tether at the start of the retrieval process, L_f is the length of the tether at the conclusion of the retrieval process, and t_R is the length of time of the retrieval process. If we substitute Eq.12 into Eqs.4–5 and integrate to find θ and ϕ, we can substitute θ, ϕ and L into Eq.3 to determine the tension induced in the tether. We can then vary the final length (L_f) after retrieval, the initial in-plane and out-of-plane angular positions ($\theta(0)$ and $\phi(0)$) and the angular velocities ($\dot{\theta}(0)$ and $\dot{\phi}(0)$) relative to the orbital plane of the system and investigate how varying these parameters affects the tension induced in the tether at the end of the retrieval process (tests of the Spectra tether to be used in TAG indicate that the breaking strength of the tether is 785 Newtons). In each case, the initial length of the tether prior to initiation of the retrieval process will be taken to be 2 kilometers and the time of retrieval, t_R, will be taken to be 20 minutes.

Fig.7 shows the tension (T_0) in the tether at the end of the retrieval (i.e. spin-up) process as a function of the parameters $\theta(0)$ and $\phi(0)$ for $\dot{\theta}(0) = \dot{\phi}(0) = 0$ for L_f=80 meters (specified in the plot descriptions). The plot shows a flat surface where the tether tension experienced is such that the 25-kg half of the satellite experiences at least "1-g" of centripetal acceleration. Fig.8 represents the same simulations as Fig.7, but shows a flat surface where the tension is such that the tether tension experienced exceeds the breaking strength (785 Newtons) of the tether. More studies of this type appear in Ref.[20] along with plots that show the tension in the tether at the end of the retrieval (i.e. spin-up) process as a function of the parameters $\dot{\theta}(0)$ and $\dot{\phi}(0)$ for $\theta(0) = \phi(0) = 0$ for various values of L_f.

The plots in Figs.7 and 8 along with the plots in Ref.[20] give an idea as to what type of mission scenarios are possible, given the material properties of the tether and the desired final centripetal acceleration. They also illustrate how the initial orientation and angular velocities of the tether axis prior to the initiation of the retrieval process affect the spin-up dynamics. These studies will help guide both satellite design and mission planning for the TAG program.

Elasticity Effects

The analysis presented here uses the "Planar Dumbbell Model with Elasticity Effects Included" equations discussed earlier. What we are investigating is how tether elasticity and the initial angular position of the system (relative to the local vertical prior to retrieval) will affect the behavior of the system during spin-up.

For the purpose of this study, we have again chosen to use a simple exponential control law for the unstretched length, L_0, of the tether (e.g. as discussed in Refs.[19] and [24]), i.e. we specify

$$L_0(t) = L_{0i} e^{-ct} \tag{10}$$

where

$$c = \frac{\ln\left(L_{0i}/L_{0f}\right)}{t_R} \tag{11}$$

and L_{0i} is the length of the tether at the start of the spin-up (retrieval) process, L_{0f} is the length of the tether at the conclusion of the spin-up process, and t_R is the length of time of the spin-up process.

We then substitute Eq.12 into Eq.6 and integrate Eqs.6 and 7 numerically to determine θ as a function of time.

For the simulations presented here we assume the following values for the orbital parameters, satellite masses, time duration of the spin-up process and the initial and final lengths of the tether prior to and after the spin-up process is complete.

$m_A = 25$ kg

$m_B = 40$ kg

$\Omega = 0.0011636$ rad/sec (90 minute orbital period)

$L_{0i} = L\left(0\right)$ =initial tether length prior to retrieval = 2000 meters

t_R = time duration for spin-up process = 90 minutes

$L_{0f} = L\left(t_R\right)$ = final tether length = 100 meters

We now simulate the spin-up dynamics for initial libration angles θ_0 ranging from -90 to +90 degrees. $\dot{\theta}_0$ is assumed to be zero at the start of the spin-up process. It should be noted that, due to space limitations, only a small sample of the rich variety of behavior observed in the simulations is presented here.

To better understand the dependence of the dynamics on tether elasticity, we first examine the way the spin-up of the entire system depends on θ_0 while neglecting the effects of tether elasticity. In Fig.9 we show the evolution of θ in the phase plane[1] as θ_0 varies from -90 to +90 degrees and time, t, varies from 0 to 5400 seconds. The complexity of the dynamics can be seen in this figure. We see from this plot that small variations in initial angle prior to spin-up can have a dramatic affect on system behavior (see also Ref.[21]). We now show what happens to the evolution of θ when the tether elasticity is accounted for. Setting $EA = 10^4$ Newtons, we show in each of Figs.10–15 two plots side-by-side to compare simulation results of the evolution of θ with time for models which assume an inelastic tether and an elastic tether, respectively; θ (in degrees) is plotted on the ordinate and time (in seconds) is plotted on the abscissa. Ref.[22] examines a wider range of possible initial angles, θ_0, but we just give a sampling here due to space limitations. From the plots we see that for $\theta_0 = 65.2^o$ there is very little change introduced in the evolution of θ when elastic effects are introduced, but at $\theta_0 = 65.4^o$, we see that the spin-up direction reverses when we introduce elasticity (note from Fig.12 that a bifurcation occurs in the phase diagram for the inelastic case between $\theta_0 = 65.0^o$ and $\theta_0 = 65.5^o$). For $\theta_0 = 69.4^o$, the direction of spin-up is again the same but there is noticeable difference in the qualitative evolution of θ. For $\theta_0 = 69.8^o$, the spin-up direction again reverses when we introduce elasticity, but when we reach $\theta_0 = 70.4^o$ there is no appreciable change in spin-up behavior when we include elastic effects.

Figs.10–15 and the plots in Ref.[22] show how initial angular position of the system (relative to the local vertical prior to initiation of spin-up) affects the spin-up dynamics of a tethered satellite system and how these effects change when the effects of tether elasticity are included. The results show that tether elasticity can significantly affect the system dynamics of a tethered satellite system during spin-up for certain sets of initial conditions. These results will help guide both satellite design and mission planning. A research program to better understand why elasticity effects figure more prominently for certain initial angular positions prior to commencement of spin-up is currently underway.

[1] See Refs.[27, 30, 32] for similar studies.

Attitude Motion of the End-Bodies

The analysis presented here uses the "Planar Inelastic Model with End-Bodies Treated as Three dimensional Objects" equations discussed earlier.

What we are investigating here is how the initial angular position of the system (relative to the local vertical prior to retrieval) will affect the behavior of the end-masses during spin-up.

For the purpose of this study, we have again chosen to use a simple exponential control law for the length L of the tether (e.g. as discussed in Refs.[19]–[24]), i.e. we specify

$$L(t) = L_i e^{-ct} \tag{12}$$

where

$$c = \frac{\ln(L_i/L_f)}{t_R}$$

and L_i is the length of the tether at the start of the spin-up (retrieval) process, L_f is the length of the tether at the conclusion of the spin-up process, and t_R is the length of time of the spin-up process.

If we substitute Eq.12 into Eq.7 and integrate to find θ, we can then substitute θ and L into Eq.6 to determine tether tension T_0. θ and T_0 can then be substituted into Eq.8 which can be integrated numerically to solve for the attitude motion β as a function of time.

For the simulations presented here we assume the following values for the orbital parameters, satellite masses, time duration of the spin-up process and the initial and final lengths of the tether prior to and after the spin-up process is complete.

$m_A = 25$ kg

$m_B = 40$ kg

$J_1 = 0.9 kg\text{–}m^2$

$J_2 = 0.9 kg\text{–}m^2$

$J_3 = 1.1 kg\text{–}m^2$

$\Omega = 0.0011636$ rad/sec (90 minute orbital period)

$L_i = L(0)$ =initial tether length prior to retrieval = 2000 meters

t_R = time duration for spin-up process = 90 minutes

$L_f = L(t_R)$ = final tether length = 100 meters

In Ref.[21], we simulate the spin-up dynamics for initial libration angles θ_0 ranging from -90 to +90 degrees. $\dot{\theta}_0$, β_0 and $\dot{\beta}_0$ are all assumed to be zero at the start of the spin-up process. in this paper, we show the attitude dynamics (represented by β) of the 40-kg End-body for the duration of the spin-up process (90 minutes, i.e. 5400 seconds) for different tether attachment points; due to space limitations, only a small sample of the rich variety of behavior observed in the simulations is presented here. In Ref.[21] a more detailed study can been found which includes the effect of different initial tether orientations as well as different tether attachment points.

Figs.16 and 17 show the evolution of $\beta(t)$ as t varies from 0 to 5400 seconds. For Figs.16 and 17, $\theta_0 = 11.8$ degrees and $\ell_2 = 20$ cm, but ℓ_1 equals 0 cm and 1 cm, respectively. Here we see a dramatic difference in the way β evolves depending on the location of the tether attachment point; in Fig.16 we see that the oscillations remain small for most of the spin-up process but grow rapidly near the end; in Fig.17, however, we have that there is a large amount of oscillation throughout the spin-up process. Hence we see that adding 1 cm of offset to the tether attachment point can change the attitude motion dramatically.

To better understand the dependence of the attitude dynamics on θ_0, we examine the way the spin-up of the entire system depends on θ_0, i.e. we again look at how $\theta(t)$ depends on θ_0. Fig.9 shows the evolution of θ in the phase plane as θ_0 varies from -90 to +90 degrees and t varies from 0 to 5400 seconds. The complexity of the dynamics can be seen in this figure, and upon observing the strong dependence of $\theta(t)$ on θ_0, we can see why β also depends strongly on θ_0 as can be seen in Ref.[21]. More detailed studies of the phase space can be found in [21]. Further investigation of the θ phase space and its influence on the attitude dynamics of the end-bodies will be presented in future work.

We have presented here, and in Ref.[21], results on how the location of the tether attachment point and the initial angular position of the system (relative to the local vertical prior to initiation of spin-up) affects the attitude motion of the end-bodies of a tethered satellite system during spin-up. The results show that system dynamics during spin-up depend strongly on initial conditions and the location of the tether attachment point. These results will help guide both satellite design and mission planning.

Summary

We have presented a brief overview of the Tethered Artificial Gravity (TAG) satellite program and have shown some of the results of our simulation studies. The mission plan calls for development of the Phase I spacecraft to be flown on the Space Shuttle in a Get-Away-Special (GAS) Canister and for the development of models of the tethered system dynamics including detailed parametric studies. Students from UTD, TCU, the Dallas-Ft. Worth area and the Beaumont area will be involved in design projects for these activities and will also develop experiments to fly on the spacecraft. The flight plan calls for launch of the Phase I spacecraft on the Space Shuttle in 2003. Planning for Phase II, which will involve the free flight of a tethered satellite system, is currently underway. The Phase II spacecraft will be a small, 65 kg, tethered satellite system which will be boosted into low-earth orbit, deployed and then spun-up to produce artificial gravity.

Acknowledgments

The authors gratefully acknowledge support from the Texas Space Grant Consortium and the Texas Higher Education Coordinating Board Advanced Research/Advanced Technology Program.

References

[1] Angrilli, F., DaForno, R., and Saggin, B., "A New Full Non-Linear Model of the Tethered Satellite System Based on the Characteristic Method, Proceedings of the Fourth International Conference on Tethers in Space, Apr 10-14, 1995, Science and Technology Corporation, Hampton, VA, pp.1299-1308.

[2] Arnold, D.A., "The Behavior of Long Tethers in Space," The Journal of the Astronautical Sciences, Vol. 35, No. 1, January-March, 1987, pp.3-18.

[3] Bainum, P. M., Bekey, I., et al, *Advances in the Astronautical Sciences, Vol. 62: Tethers in Space*, AAS Publications, 1987.

[4] Bainum, P. M., and Evans, K. S., "Gravity-Gradient Effects on the Motion of Two Rotating Cable-Connected Bodies, AIAA Journal, Vol. 14, No. 1, Jan, 1976, pp.26-31.

[5] Bainum, P.M., and Evans, K.S., "Three-Dimensional Motion and Stability of Two Rotating Cable-Connected Bodies," J. Spacecraft, Vol. 12, No. 4, April 1975, pp.242-250.

[6] Bainum, P. M., and Kumar, V. K., "Optimal Control of the Shuttle-Tethered-Subsatellite System, Acta Astronautica, Vol. 7, 1980, pp.1333-1348.

[7] Beletsky, V. V., and Levin, E. M., *Advances in the Astronautical Sciences, Vol. 83: Dynamics of Space Tether Systems*, AAS Publications,1993.

[8] Charles, J., "The physiological effects of long duration space flight,", NASA Johnson Space Center, *Presentation at the Texas Space Grant Consortium Meeting*, Austin, TX, Nov. 2000.

[9] Chobotov, V., "Gravity-Gradient Excitation of a Rotating Cable-Counterweight Space Station in Orbit," Journal of Applied Mechanics, December 1963, pp.547-554.

[10] Cosmo, M. L., and Lorenzini, E. C., *Tethers in Space Handbook*, NASA Marshall Space Flight Center and the Smithsonian Astrophysical Observatory, 1997.

[11] Grassi, M. and Cosmo, M.L., "Attitude Dynamics of the Small Expendable-Tether Deployment System," Acta Astronautica, Vol. 36, No.3, 1995, pp.141-148.

[12] James, H.G., Yau, A.W., et al, "Space Research in the Biceps Experiment," Proceedings of the Fourth International Conference on Tethers in Space, Vol. III, Apr 10-14, 1995, Science and Technology Corporation, Hampton, VA, pp.1585-1597.

[13] Kalantzis, S., Modi, V.J., Pradhan, S., Misra, A. K., "Order-N Formulation and Dynamics of Multibody Tethered Systems", Journal of Guidance, Control, and Dynamics, Vol. 21, No. 2, March-April, 1998, pp. 277-285.

[14] Keshmiri, M., and Misra, A.K., "General Formulation for N-Body Tethered Satellite System Dynamics," Journal of Guidance, Control and Dynamics, Vol. 19, No. 1, January-February, 1996, pp.75-83.

[15] Lorenzini, E.C., Bortolami, S.B., et al, "Control and Flight Performance of Tethered Satellite Small Expendable Deployment System-II," Journal of Guidance, Control and Dynamics, Vol. 19, No. 5, September-October, 1996, pp.1148-1156.

[16] Luongo, A., and Vestroni, F., "Non-linear Free Periodic Oscillations of a Tethered Satellite System, Journal of Sound and Vibration, Vol. 175, No. 3, 1994, pp.299-315.

[17] Mazzoleni, A. P., Coles, R. L., "A Study of the Deployment Dynamics of the ASTOR Tethered Satellite System" *Proceedings of the 1999 AAS/AIAA Astrodynamics Conference, Girdwood, Alaska, August 16-18* (AAS Paper 99-414).

[18] Mazzoleni, A. P., "Nonplanar Deployment Dynamics of the ASTOR Tethered Satellite System", *Proceedings of the 2000 AAS/AIAA Space Flight Mechanics Meeting, January 23-26, Clearwater, FL, January 23 26* (AAS Paper 00-187).

[19] Mazzoleni, A. P., "Dynamics of a Tethered Satellite Technology Demonstrator During Spin-Up", *Proceedings of the 51st international Astronautical Congress, Rio de Janeiro, Brazil, October 2–6, 2000* (Paper IAF-00-I.2.09).

[20] Mazzoleni, A. P. and Hoffman, J. H., "Nonplanar Spin-Up Dynamics of the ASTOR Tethered Satellite System", *Proceedings of the 2001 AAS/AIAA Space Flight Mechanics Meeting, Santa Barbara, CA, February 11-15* (AAS Paper 01-193).

[21] Mazzoleni, A. P., Hoffman, J. H.,"Attitude Dynamics of the End-Bodies of a Tethered Satellite System During Spin-Up" *Proceedings of the 2001 AAS/AIAA Astrodynamics Conference, Quebec City, July 30 August 2* (AAS Paper 01-402).

[22] Mazzoleni, A. P., Hoffman, J. H.,"Effects of Tether Elasticity on the Spin-Up Dynamics of a Tethered Satellite System," presented at the *Astrodynamics Symposium of the 52nd International Astronautical Congress, Toulouse, France, October 1-5, 2001* (Paper IAF-01-A.4.05).

[23] Misra, A. K., and Modi, V.J., "Deployment and Retrieval of Shuttle Supported Tethered Satellites," Journal of Guidance, Control and Dynamics, Vol. 5, No. 3, May-June, 1982, pp.279–285.

[24] Misra, A. K., and Modi, V.J., "A Survey on the Dynamics and Control of Tethered Satellite Systems, *Advances in the Astronautical Sciences, Vol. 62: Tethers in Space*, AAS Publications, 1987, pp.667-720.

[25] Modi, V.J., Pradhan, S., et al, "Experimental Investigation of the Dynamics of Spinning Tethered Bodies," Acta Astronautica, Vol. 39, No.7, 1996, pp.487-495.

[26] Modi, V.J. and Misra, A.K., "On the Deployment Dynamics of Tether Connected Two-Body Systems," Acta Astronautica, Vol. 6, 1979, pp.1183-1197.

[27] " Nonlinear Dynamics and Chaos of Two-Body Tethered Satellite Systems", Nixon, M.S. and Misra, A.K., Advances in the Astronautical Sciences, Proceedings of the AAS/AIAA Astrodynamics Conference. Part 1 (of 3), Aug 16-19 1993, 1993, Victoria, BC, pp.775-794.

[28] No, T.S., and Cochran, J.E., Jr., "Dynamics and Control of a Tethered Flight Vehicle," Journal of Guidance, Control and Dynamics, Vol. 18, No. 1, January-February, 1995, pp.66-72.

[29] Paul, B., "Planar Librations of an Extensible Dumbbell Satellite, AIAA Journal, Vol. 1, No. 2, Dec, 1968, pp.411-418.

[30] Pelaez, J., "On the Dynamics of the Deployment of a Tether from an Orbiter–Part II. Exponential Deployment," Acta Astronautica, Vol. 36, No.6, 1995, pp.313-335.

[31] Pelaez, J., and Lorenzini, E.C., "Sensitivity Analysis of Tether-Mediated Orbital Injection," Journal of the Astronautical Sciences, Vol. 44, No. 4, Oct-Dec, 1996, pp.491-514.

[32] Pines, D. J., von Flotow, A. H. and Redding, D. C., "Two Nonlinear Control Approaches for Retrieval of a Thrusting Tethered Subsatellite," Journal of Guidance, Control and Dynamics, Vol. 13, No. 4, July-August, 1990, pp.651-658.

[33] Pradhan, S., Modi, V.J., and Misra, A.K., "On the Offset Control of Flexible Nonautonomous Tethered Two-Body Systems," Acta Astronautica, Vol. 38, No.10, 1996, pp.783-801.

[34] Quadrelli, B. M., and Lorenzini, E. C., "Dynamics and Stability of a Tethered Centrifuge in Low Earth Orbit", *Journal of the Astronautical Sciences*, Vol. 40 No.1, Jan-Mar, 1992, pp.3-25.

[35] Robe, T. R., "Stability of Two Tethered Unsymmetrical Earth-Pointing Bodies, AIAA Journal, Vol. 6, No. 12, Dec, 1968, pp.2282-2288.

[36] Santangelo, A.D., Onsager, T.G., and Kletzing, C.A., "Airseds-I: A Proof-of-Concept Tether Mission into the Earth's Upper Atmosphere," Proceedings of the Fourth International Conference on Tethers in Space, Vol.III, Apr 10-14, 1995, Science and Technology Corporation, Hampton, VA, pp.1527-1541.

[37] Santangelo, A.D., "Airseds-II: A TSS-2 Precursor Mission to Test and Demonstrate Tethered Systems in the Earth's Upper Atmosphere," Proceedings of the Fourth International Conference on Tethers in Space, Vol. III, Apr 10-14, 1995, Science and Technology Corporation, Hampton, VA, pp.1675-1684.

[38] Schechter, H. B., "Dumbbell Librations in Elliptic Orbits, AIAA Journal, Vol. 2, No. 6, Dec, 1968, pp.1000-1003.

[39] Schultz, D. N. et al.,"A Manned Mars Artificial Gravity Vehicle", *Proceedings of the Second International Conference on Tethers in Space*, Oct.4 8, 1987, Venice, Italy, pp.320-335.

[40] Singh, R.B., "Three-Dimensional Motion of a System of two Cable-Connected Satellites in Orbit," Acta Astronautica, Vol. 18, No.5, 1973, pp.301-308.

[41] Thornburg, Shannon L. and Powell, J. David, "Thrusterless Vibration Control for Tethered Artificial Gravity Spacecraft", *Advances in the Astronautical Sciences, Vol. 85, AAS Publications*, 1994 pp.839-885.

[42] Tyc, G., and Han, R. P. S., "Attitude Dynamics Investigation of the Oedipus-A Tethered Rocket Payload, Journal of Spacecraft and Rockets, Vol. 32, No. 1, Jan-Feb, 1995, pp.133-141.

[43] Vigneron, F.R., Jablonski, A.M., et al, "Comparison of Analytical Modeling of OEDIPUS Tethers with Data from Tether Laboratory," Journal of Guidance, Control and Dynamics, Vol. 20, No. 3, May-June, 1997, pp.471-478.

[44] Vigneron, F.R., Jablonski, A.M., et al, "Validation of Analytical Modeling of Oedipus Tethers Using Experimental Results from Te-Lab," Proceedings of the Fourth International Conference on Tethers in Space, Vol. III, Apr 10-14, 1995, Science and Technology Corporation, Hampton, VA, pp.1483-1497.

[45] von Flotow, A.H., and Williamson, P.R., "Deployment of a Tethered Satellite Pair Into Low Earth Orbit for Plasma Diagnostics," The Journal of the Astronautical Sciences, Vol. 34, No. 1, January-March, 1986, pp.65-90.

Figures

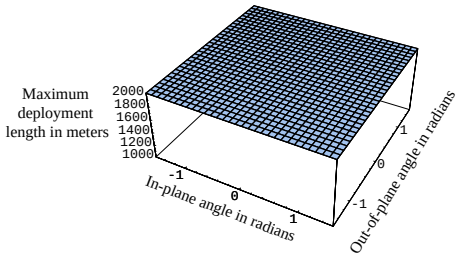

Figure 1: Final Deployed Length as a function of alignment with the local vertical prior to deployment for $T_0 = 50$ mN, $m_A = 25$ kg and $\dot{L}(0) = 5.0$ m/sec.

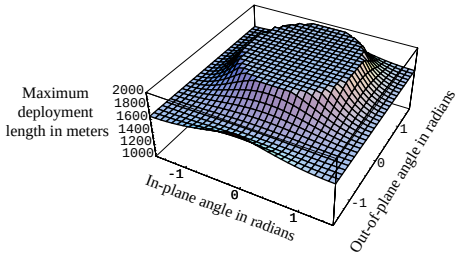

Figure 2: Final Deployed Length as a function of alignment with the local vertical prior to deployment for $T_0 = 100$ mN, $m_A = 25$ kg and $\dot{L}(0) = 5.0$ m/sec.

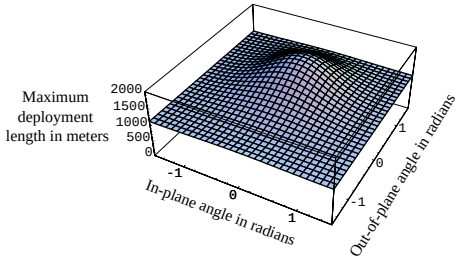

Figure 3: Final Deployed Length as a function of alignment with the local vertical prior to deployment for $T_0 = 100$ mN, $m_A = 25$ kg and $\dot{L}(0) = 4.0$ m/sec.

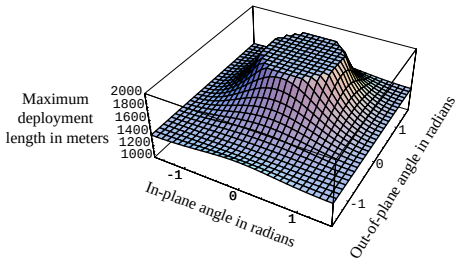

Figure 4: Final Deployed Length as a function of alignment with the local vertical prior to deployment for $T_0 = 100$ mN, $m_A = 25$ kg and $\dot{L}(0) = 4.5$ m/sec.

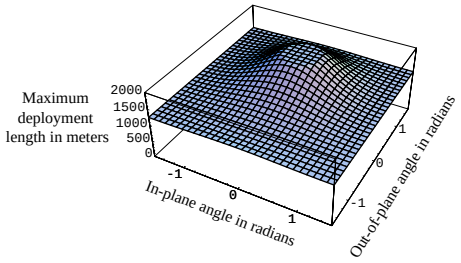

Figure 5: Final Deployed Length as a function of alignment with the local vertical prior to deployment for $T_0 = 100$ mN, $m_A = 20$ kg and $\dot{L}(0) = 4.5$ m/sec.

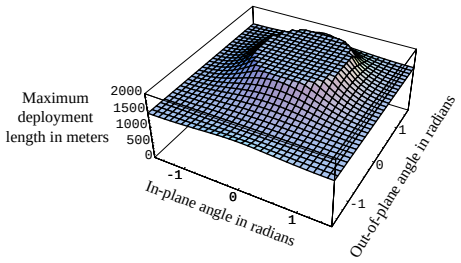

Figure 6: Final Deployed Length as a function of alignment with the local vertical prior to deployment for $T_0 = 100$ mN, $m_A = 30$ kg and $\dot{L}(0) = 4.5$ m/sec.

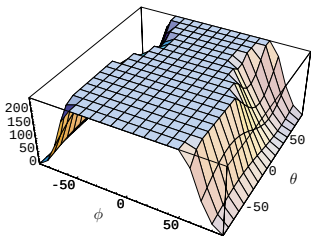

Figure 7: Tension in tether (in Newtons) at end of spin-up (final tether length = 80 meters) vs. initial in-plane (θ) and out-of-plane (ϕ) angles, assuming $\dot{\theta}(0) = \dot{\phi}(0) = 0$. Note: Flat region indicates Tension is such that the 25 kg half of satellite experiences at least $1 - g$ of centripetal acceleration.

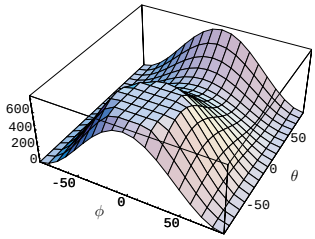

Figure 8: Tension in tether (in Newtons) at end of spin-up (final tether length = 80 meters) vs. initial in-plane (θ) and out-of-plane (ϕ) angles, assuming $\dot{\theta}(0) = \dot{\phi}(0) = 0$. Note: Flat region indicates Tension exceeds failure limit of the tether.

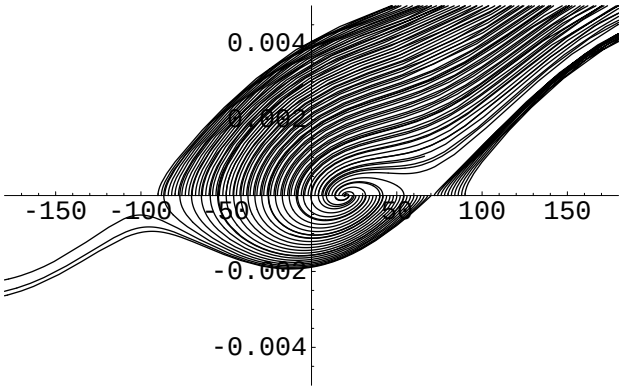

Figure 9: Phase Plane Evolution of $\theta(t)$ as t varies from 0 to 5400 seconds; θ_0 varies from -90 to +90 degrees. (θ is plotted on the abscissa and $\dot{\theta}$ (in radians per second) is plotted on the ordinate).

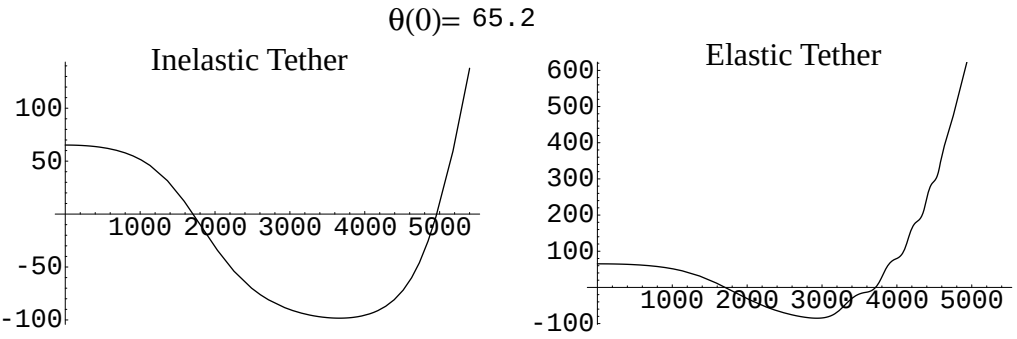

Figure 10: Comparison of Evolution of θ with time for models which assume an inelastic tether and an elastic tether, respectively ($\theta_0 = 65.2$ degrees). θ (in degrees) is plotted on the ordinate and time (in seconds) is plotted on the abscissa.

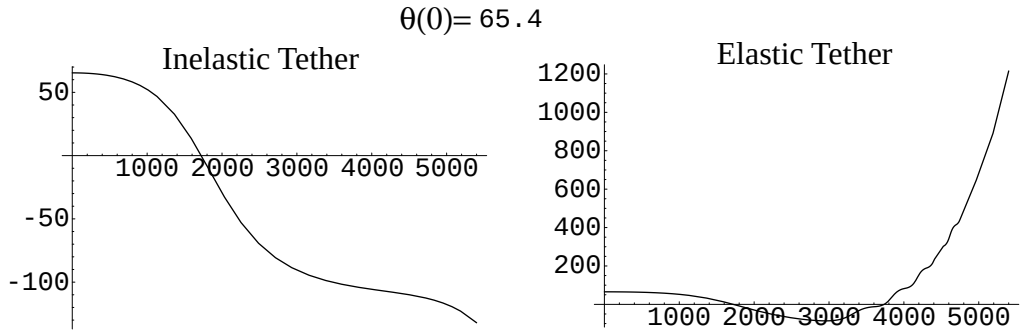

Figure 11: Comparison of Evolution of θ with time for models which assume an inelastic tether and an elastic tether, respectively ($\theta_0 = 65.4$ degrees). θ (in degrees) is plotted on the ordinate and time (in seconds) is plotted on the abscissa.

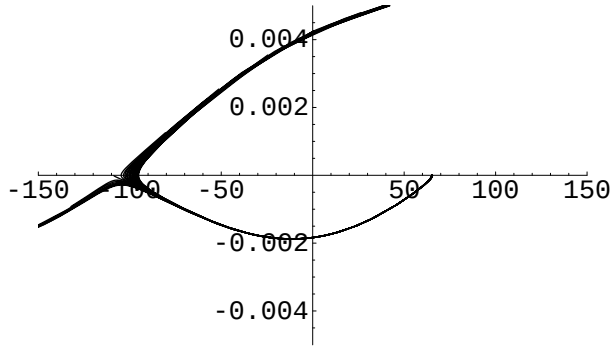

Figure 12: Phase Plane Evolution of $\theta(t)$ (neglecting tether elasticity) as t varies from 0 to 5400 seconds; θ_0 varies from 65 to 65.5 degrees. (θ is plotted on the abscissa and $\dot{\theta}$ (in radians per second) is plotted on the ordinate).

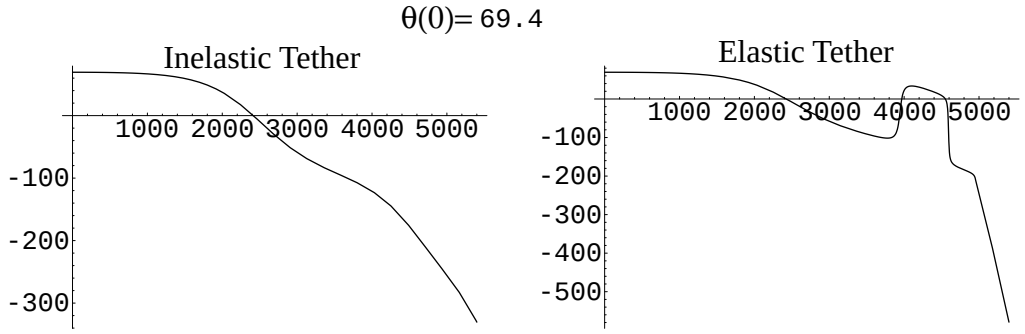

Figure 13: Comparison of Evolution of θ with time for models which assume an inelastic tether and an elastic tether, respectively ($\theta_0 = 69.4$ degrees). θ (in degrees) is plotted on the ordinate and time (in seconds) is plotted on the abscissa.

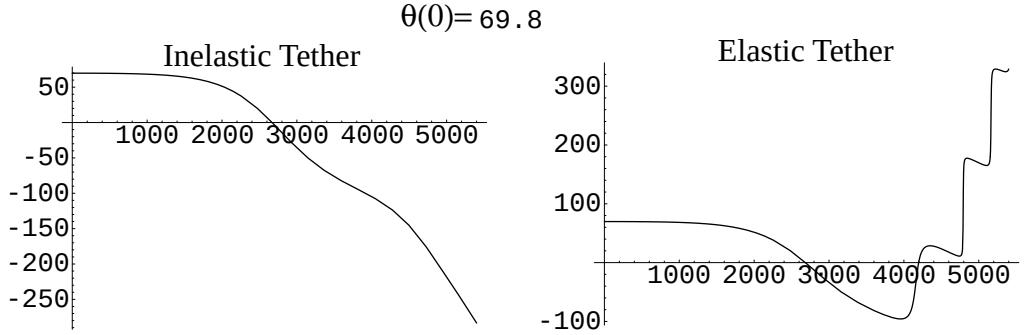

Figure 14: Comparison of Evolution of θ with time for models which assume an inelastic tether and an elastic tether, respectively ($\theta_0 = 69.8$ degrees). θ (in degrees) is plotted on the ordinate and time (in seconds) is plotted on the abscissa.

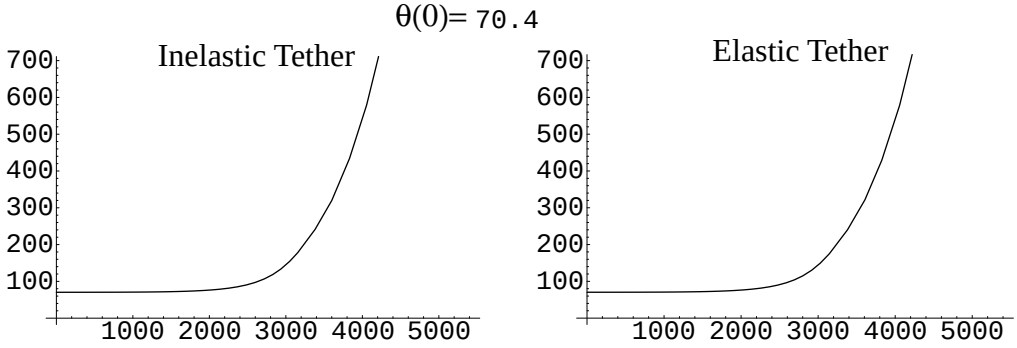

Figure 15: Comparison of Evolution of θ with time for models which assume an inelastic tether and an elastic tether, respectively ($\theta_0 = 70.4$ degrees). θ (in degrees) is plotted on the ordinate and time (in seconds) is plotted on the abscissa.

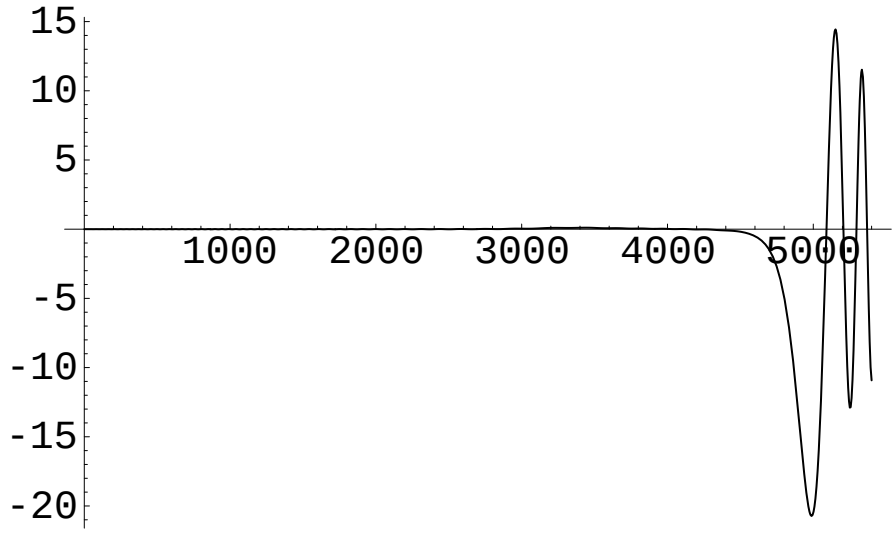

Figure 16: Attitude Dynamics, β (in degrees), during Spin-Up, as t varies from 0 to 5400 seconds; $\ell_3 = 20$ cm, $\theta_0 = 11.8$ degrees and $\ell_1 = 0$ cm.

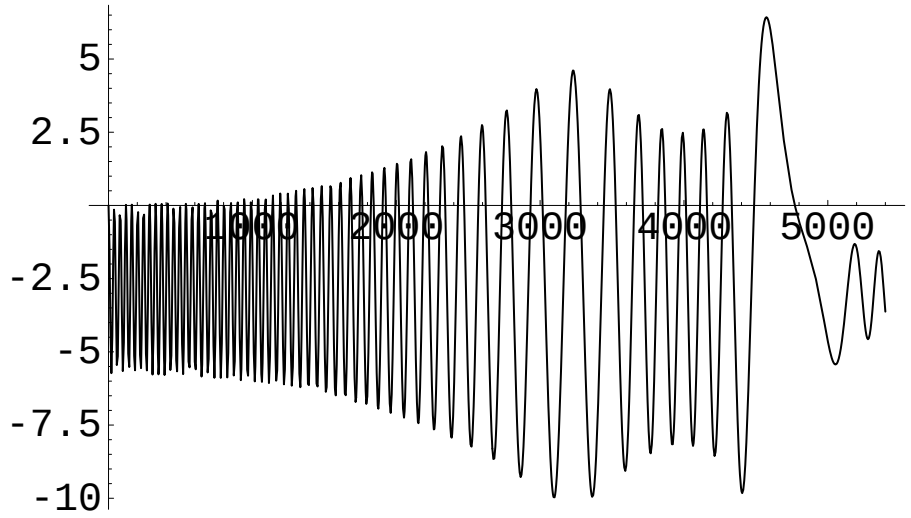

Figure 17: Attitude Dynamics, β (in degrees), during Spin-Up, as t varies from 0 to 5400 seconds; $\ell_3 = 20$ cm, $\theta_0 = 11.8$ degrees and $\ell_1 = 1$ cm.